

**A case study in
megacity Beijing,
China**

X. Liu et al.

This discussion paper is/has been under review for the journal Atmospheric Chemistry and Physics (ACP). Please refer to the corresponding final paper in ACP if available.

Formation and evolution mechanism of regional haze: a case study in the megacity Beijing, China

X. Liu^{1,2}, J. Li³, Y. Qu⁴, T. Han¹, L. Hou¹, J. Gu², C. Chen², Y. Yang¹, X. Liu⁵,
T. Yang⁴, Y. Zhang², H. Tian¹, and M. Hu²

¹State Key Laboratory of Water Environment Simulation, School of Environment, Beijing Normal University, Beijing 100875, China

²State Key Joint Laboratory of Environment Simulation and Pollution Control, College of Environmental Sciences and Engineering, Peking University, Beijing 100871, China

³College of Civil Aviation, Nanjing University of Aeronautics and Astronautics, Nanjing 210016, China

⁴State Key Laboratory of Atmospheric Boundary Layer Physics and Atmospheric Chemistry, Institute of Atmospheric Physics, Chinese Academy of Sciences, 100029, China

⁵School of Physics, Peking University, Beijing 100871, China

Received: 18 April 2012 – Accepted: 12 June 2012 – Published: 3 July 2012

Correspondence to: X. G. Liu (liuxingang@bnu.edu.cn) and M. Hu (minhu@pku.edu.cn)

Published by Copernicus Publications on behalf of the European Geosciences Union.

Title Page

Abstract

Introduction

Conclusions

References

Tables

Figures

◀

▶

◀

▶

Back

Close

Full Screen / Esc

Printer-friendly Version

Interactive Discussion



Abstract

The main objective of this study is to investigate the formation and evolution mechanism of the regional haze in megacity Beijing by analyzing the process of a severe haze that occurred 20–27 September 2011. Mass concentration and size distribution of aerosol particles as well as aerosol optical properties were concurrently measured at the Beijing urban atmospheric environment monitoring station. Gaseous pollutants (SO_2 , NO - NO_2 - NO_x , O_3 , CO) and meteorological parameters (wind speed, wind direction, and relative humidity (RH)) were simultaneously monitored. Meanwhile, aerosol spatial distribution and the height of planetary boundary layer (PBL) were retrieved from the signal of satellite and LIDAR (light detection and ranging). Results showed that high intensity of local pollutants from Beijing urban source is the fundamental cause that led to the regional haze. Meteorological factors such as higher RH, weak surface wind speed, and decreasing height of PBL played an important role on the deterioration of air quality. New particle formation was considered to be the most important factor contributing the formation of haze. In order to improve the atmospheric visibility and reduce the occurrence of the haze, the mass concentration of $\text{PM}_{2.5}$ at dry condition should be less than $60 \mu\text{g m}^{-3}$ in Beijing according to the empirical relationship of visibility, $\text{PM}_{2.5}$ mass concentration and RH. This case study may provide valuable information for the public to recognize the formation mechanism of the regional haze event over the megacity, which is also useful for the government to adopt scientific approach to forecast and eliminate the occurrence of regional haze in China.

1 Introduction

Airborne aerosols, such as sulfate, nitrate, ammonium, particulate organic matter, black carbon, and other chemical species, can scatter and absorb the incident light and therefore lead to atmosphere opacity and horizontal visibility degrade. When the horizontal visibility is equal to or less than 10 km and atmospheric relative humidity (RH) is equal

A case study in megacity Beijing, China

X. Liu et al.

Title Page

Abstract

Introduction

Conclusions

References

Tables

Figures

⏪

⏩

◀

▶

Back

Close

Full Screen / Esc

Printer-friendly Version

Interactive Discussion



A case study in megacity Beijing, China

X. Liu et al.

Title Page

Abstract

Introduction

Conclusions

References

Tables

Figures

◀

▶

◀

▶

Back

Close

Full Screen / Esc

Printer-friendly Version

Interactive Discussion

to or less than 90 %, this phenomenon is called atmospheric haze (Wu et al., 2006). Haze is pollution of fine particles in nature; fine particles are mainly from industrial emissions, vehicle exhaust pollutants, and secondary aerosols formed through a series of photochemical reactions. Haze has adverse effects on human health (Yadav et al., 2003; Xiao et al., 2006; Bell et al., 2011). Haze, rich in toxic and hazardous substances, can directly enter the human body through the respiratory system and adhere to the upper and lower respiratory tract and lungs, which ultimately causes respiratory and cardiovascular diseases (Tie et al., 2009). In addition, haze reduces visibility and could directly affect the land, sea and air traffic safety (Wu et al., 2005; Mukherjee and Viswanathan, 2001). Haze has also been found to have impact on natural and agricultural ecosystems. For example, haze, a higher concentration of atmospheric particles absorbing and scattering the incident sunlight, results in the decreasing intensity of solar radiation and sunshine hours, thus leading to the reduction of agricultural production and disruption of ecosystems (Chameides et al., 1999).

Historically, haze has occurred in some areas of the United Kingdom and the United States due to their developed economies (McNulty, 1968; Lee, 1983; Schichtel et al., 2001). Till now, haze frequently has occurred in the regions of North Africa, Indian Ocean, and Asia (Quinn and Bates, 2003; Huebert et al., 2003). Scientists throughout the world have carried out many experiments to understand the formation mechanism of haze and governments have taken effective measures to reduce the occurrence of haze (Huebert et al., 2003; Zhang et al., 2004; Wu et al., 2005; Malm and Day, 2001; Wang et al., 2006). The United States carried out observations of atmospheric visibility and launched a large-scale visibility observation program IMPROVE (Interagency Monitoring of Protected Visual Environment Program), which established a visibility monitoring network in 1988 (Malm and Day, 2001). Furthermore, the United States developed and adopted Regional Haze Rule in 1999 (<http://www.epa.gov/>) calling for state and federal agencies to work together to improve visibility. Also in 1999, scientists found that the northern Indian Ocean, South and Southeast Asia were shrouded

by the atmospheric brown haze during the INDOEX (Indian Ocean Experiment) (Quinn et al., 2002).

In the past 30 yr, with the rapid economic and social development, many cities in China have suffered from air pollution and extremely haze because of heavy dispersion of air pollutants (Wu et al., 2006). When haze happens, the sky seems cloudy, blurry and poorly visible to the people. Haze episodes have been now characterized by increasing frequencies, longer duration and expanding sphere. Haze, as well as its adverse effects, is one of the most concerned problems in China, and it has become the major air quality issue at the moment. There are four major haze polluted areas in China: Jing-Jin-Tang Region, the Yangtze River Delta, Sichuan Basin and the Pearl River Delta (PRD), among which, the PRD is the area coupled with the most frequently occurring haze episodes. Taking Guangzhou, the central city in PRD as an example, the number of haze days was 70 in 2001; 83 days in 2002; 93 days in 2003; and 144 days in 2004 (Wu et al., 2006; Deng et al., 2008). An extreme haze event happened on 2 November 2003 in Guangzhou with the instantaneous visibility value less than 200 m, reported by Wu et al. (2005). Low visibilities due to aerosol pollution and high RH have been also observed in Xinken and Guangzhou during two PRD campaigns (Cheng et al., 2006, 2008a, b; Liu et al., 2008). The number of hazy days in Beijing urban area was 17 days in 1971, sharply grew to 223 days in 1982, and kept this level (~200 days) until 1998 (Yang, 2008). Since 1998, Beijing has had vigorously implemented a number of measures focusing on management of coal, motor vehicles, industrial and dust pollution to improve air quality (Sun et al., 2004). As a result, the hazy days quickly decreased to 73 days in 2005. But, in 2011, the haze in megacity Beijing had increased in intensity, and this extreme heavy haze could have significantly adverse effects on human health.

Haze has been studied by scientists at home and abroad during the past two decades (Chen et al., 2003). Chen et al. (2003) studied the formation and evolution mechanism of summertime haze in the mid-Atlantic region and signified the role of stationary weather conditions, RH in the haze formation and also clarified that secondary

A case study in megacity Beijing, China

X. Liu et al.

Title Page

Abstract

Introduction

Conclusions

References

Tables

Figures



Back

Close

Full Screen / Esc

Printer-friendly Version

Interactive Discussion



A case study in megacity Beijing, China

X. Liu et al.

Title Page

Abstract

Introduction

Conclusions

References

Tables

Figures

◀

▶

◀

▶

Back

Close

Full Screen / Esc

Printer-friendly Version

Interactive Discussion



aerosol ammoniated sulfate was most responsible for summertime haze at this locale. IMPROVE results suggested that haze is often regional in nature (Malm and Day, 2001). However, the formation and evolution of a haze is complicated, involving the formation, growth, transport, and dispersion of aerosols (Chen et al., 2003). Most of haze has occurred in the developed region in China and resulted from excess particulate matter emitted by anthropogenic sources and gas-to-particle conversion (Sun et al., 2006; Wu et al., 2005; Wang et al., 2006; Du et al., 2011). Regional haze has happened frequently especially during cold winter and spring seasons because of the enhanced heating/traffic/industrial emissions with the stable synoptic conditions (Wang et al., 2006; Sun et al., 2006). Du et al. (2011) classified the haze happening in Shanghai in summertime as biomass burning-induced, complicated, and from secondary pollutions according to its formation mechanism. But, dust-storms, which mostly happen in northern China in spring season, has a special haze due to the transported dust with high wind speed. However, available studies on the haze mostly focused on the chemical compositions of aerosols and scarcely on the formation and evolution mechanism of the haze (Sun et al., 2006; Wu et al., 2005; Wang et al., 2006; Du et al., 2011; Cheng et al., 2006, 2008a, b; Liu et al., 2008; Yang, 2008). Therefore, studies on the formation and evolution mechanism of regional haze would be useful for air quality forecast and would provide scientific support for the government to take effective measures to reduce the incidence of regional haze.

2 Experiment

2.1 Experiment site

The measurements were carried out in Beijing, the capital of the People's Republic of China, and the national center for politics, culture, and international business. The city's population is 36 million and its population density is 7837 people per km² as of 2010, more than the densely populated Greater London (5437 people per km²)

and Tokyo (5984 people per km²) (http://www.chinadaily.com.cn/bizchina/2011-07/19/content_12930151.htm). Furthermore, the total energy consumption is 69.5 million tons of standard coal, and there are more than 4.8 million cars in Beijing as of 2010 (<http://www.bjstats.gov.cn/nj/main/2011-tjnj/index.htm>). High degrees of population density and economic level have unavoidably resulted in heavy emission of air pollutants in Beijing.

Field measurements from 20–27 September were carried out at the Peking University (PKU) urban atmospheric environment monitoring station (39.98° N, 116.35° E), which lies in the northwestern part of Beijing and is ~600 m to the north of the 4th ring road that acts as one of the main traffic lines of Beijing. The observation site is located on the roof of a 6-floor building (~20 m above ground level); all of the instruments were installed in an air-conditioned room except the visibility sensor, which was installed outdoors. Possible air pollutant sources arriving at measurement site were local vehicular traffic, combustion of fuels for cooking, and some of the transported pollutants.

2.2 Measurements

The instruments involved in this study are listed in Table 1. Mass concentration of PM_{2.5} (particulate matter with aerodynamic diameter of less than 2.5 μm) was monitored by TEOM (Tapered element oscillating microbalance). Gaseous pollutants (SO₂, NO-NO₂-NO_x, O₃, CO) were detected by i-series automatic monitoring system manufactured by Thermo Electron Corporation (USA). Meteorological parameters including wind speed and RH were measured by the automatic meteorological station. Particle size distribution was measured by SMPS (Scanning Mobility Particle Sizers) and APS (Aerodynamic Particle Sizer) (Liu et al., 2008). The SMPS spectrometer is a system that measures the particle number size distribution in the size range from 2.5 to 1000 nm. Particles of different sizes were classified with differential mobility analyzer (DMA), and their concentrations were measured with a condensation particle counter

A case study in megacity Beijing, China

X. Liu et al.

Title Page

Abstract

Introduction

Conclusions

References

Tables

Figures

⏪

⏩

◀

▶

Back

Close

Full Screen / Esc

Printer-friendly Version

Interactive Discussion



(CPC). The APS measured particle size distributions with aerodynamic diameters from 0.5 to 20 μm .

The nephelometer continuously measured the light scattering coefficient by dry particles σ_{sp} (dry) at a wavelength of 532 nm. A silicone tube drier maintained the RH of the pumped air less than <30% during the field study. The nephelometer was routinely calibrated by zero and span check. The nephelometer correction factor for truncation error had been done by Liu et al. (2008). The MAAP (Petzold and Schönlinner, 2004) operated at the incident light wavelength of 670 nm on the principle of light attenuation due to absorption by aerosols deposited on the quartz fiber filter. Aerosol absorption coefficient was then calculated by the product of mass concentration of BC by specific absorption coefficient ($6.6 \text{ m}^2 \text{ g}^{-1}$), which was from the manufacture guide. Spectral aerosol optical depth (AOD) was measured by a 5-channel (380, 500, 675, 870, and 1020 nm) handheld sunphotometer (Microtops Π , USA). The instrument is equipped with five accurately aligned optical collimators. Each channel is fitted with a narrow-band interference filter and a photodiode suitable for the particular wavelength range. Radiation captured by the collimator and filtered onto the photodiodes produces an electrical current that is proportional to the radiant power. AOD is determined by the Bouguer-Lambert-Beer law. Additionally, in order to investigate the sources of the regional haze from a large scale, spatial distribution of AOD with 10 km \times 10 km resolution was retrieved from the remote sensing data of the Moderate Resolution Imaging Spectroradiometer (MODIS) on Terra and Aqua satellites (<http://modis-atmos.gsfc.nasa.gov/>).

Visibility sensor system consisted of a transmitter, a receiver, and a controller. It measured the light extinction of infrared light ($\lambda = 875 \text{ nm}$) in air, and the measurement range was from 10 m to 50 km. It should be noted that the wavelengths that the optical instruments used were different, so all parameters were scaled to values at the wavelength of 550 nm by using a power-law wavelength dependence (i.e., with the help of Ångström exponents that were retrieved from the spectral distribution of AOD). The measured value of visibility was directly transformed to atmospheric

A case study in megacity Beijing, China

X. Liu et al.

Title Page

Abstract

Introduction

Conclusions

References

Tables

Figures

◀

▶

◀

▶

Back

Close

Full Screen / Esc

Printer-friendly Version

Interactive Discussion



extinction coefficient σ_{ext} (RH) at 550 nm in unit of inverse megameter (Mm^{-1}) by Eq. (1) (Koschmieder, 1924; Seinfeld and Pandis, 2006):

$$\sigma_{\text{ext}}(\text{RH}) = \frac{3.912 \times 10^3}{\text{Vis}} \times \frac{550}{\lambda}. \quad (1)$$

The LIDAR (light detection and ranging), being similar to that reported by Sugimoto et al. (2009), was installed in the institute of atmospheric physics (IAP), Chinese academy of sciences (39.98° N, 116.37° E), about 5.7 km east of Peking University. The same conditions of PBL were assumed at these two nearby measurement sites. The LIDAR was designed for automated continuous operation and was directed vertically. The LIDAR was operated for 5 min every 15 min, and the averaged profile data were stored. Therefore, 96 profiles were recorded per day. The LIDAR had a 25-MHz analog-to-digital conversion rate, which means a 6 m height resolution. LIDAR signals were processed with range corrected and overlap corrected, and then the calibrated signals could be used to retrieve the height of planetary boundary layer (PBL). Several methods, including threshold techniques (Melfi et al., 1985) and gradient techniques (Hayden et al., 1997), have been investigated to extract the PBL height from LIDAR data. The fundamental premise took advantage of the large variance in aerosol echo profile where the aerosol concentration changed abruptly between the free troposphere and mixing layer. In this study, we used the coefficient of variance of LIDAR signals calculated by Eq. (2) to detect the height of the PBL:

$$v = \frac{S}{\bar{X}} \times 100\% = \frac{\sqrt{\frac{n \sum_{i=1}^n (x_i - \bar{x})^2}{n}}}{\sum_i 1^n x_i} \times 100\% \quad (2)$$

where S is standard deviation and \bar{x} is the average of adjacent five LIDAR signals, which were from the normalized backscattering data on 532 nm wavelength channel. The site where its coefficient of variance is the maximum is the height of the PBL.

A case study in megacity Beijing, China

X. Liu et al.

Title Page

Abstract

Introduction

Conclusions

References

Tables

Figures

◀

▶

◀

▶

Back

Close

Full Screen / Esc

Printer-friendly Version

Interactive Discussion



3 Results and discussion

3.1 Process of regional haze

3.1.1 Temporal variations of atmospheric pollutants

Temporal variations of measured NO, NO₂, SO₂, O₃, CO, and PM_{2.5} in Beijing from 20–27 September 2011 are depicted in Fig. 1. Generally, the concentrations of air pollutants NO₂, SO₂, CO, and PM_{2.5} had an increasing trend, with the exception of NO, probably due to the scavenging process by O₃. O₃, which is formed by photochemical reactions between volatile organic compounds (VOCs) and nitrogen oxides (NO_x) in the presence of heat and sunlight (Seinfeld and Pandis, 2006), also showed an increasing trend until 24 September with a slight decrease on 25 and 26 September. O₃ concentration in this pollution episode exceeded 100 ppbV and reached 120 ppbV on 24 September, which was higher than the national ambient air quality standards for O₃ (93 ppbV) (i.e., China air quality standard 200 µg m⁻³). Pollutants SO₂, NO₂ and CO, being the emissions from biomass, fuel and coal burning, had the same increasing trend from 20–27 September. The mass loading of PM_{2.5} gradually accumulated, and its instantaneous value reached at 220 µg m⁻³ at midnight of 26 September and daily average was 143 µg m⁻³ on 26 September, which was nearly 4 times as high as the daily limit (35 µg m⁻³) of the USA Ambient Air Quality Standard. Sun et al. (2004) monitored an extreme PM_{2.5} concentration with 349 µg m⁻³ in winter from 2002 to 2003, and He et al. (2001) monitored extreme PM_{2.5} concentration with 357 µg m⁻³ in Beijing from July 1999 to September 2000. Concentrations of NO, NO₂, SO₂, O₃, CO, and PM_{2.5} observed in this study had exceeded the national ambient air quality standards for residents, indicating that air pollution had been very serious, and such a high value of PM_{2.5} was regularly considered unsuitable for residents.

A case study in megacity Beijing, China

X. Liu et al.

Title Page

Abstract

Introduction

Conclusions

References

Tables

Figures

◀

▶

◀

▶

Back

Close

Full Screen / Esc

Printer-friendly Version

Interactive Discussion



3.1.2 Temporal variations of atmospheric optical properties

Figure 2 shows the temporal series of observed aerosol scattering coefficient σ_{sp} , aerosol absorption coefficient σ_{ap} , absorption coefficient by NO_2 σ_{ag} , atmospheric extinction coefficient σ_{ext} , and atmospheric visibility (Vis) in Beijing from 20–27 September 2011. Absorption coefficient by NO_2 σ_{ag} was calculated by experiential equation $\sigma_{ag} = 0.33 \cdot [\text{NO}_2]$ from Hodkinson (1966). σ_{sp} , σ_{ap} , and σ_{ext} had the same tendency to increase in the formation process of haze. Furthermore, the value of σ_{ext} was nearly 5600 Mm^{-1} in the morning of 26 September and the corresponding visibility was only 1.1 km. σ_{ag} also had an increasing trend with apparent diurnal variation. The visibility decreased sharply from 23 September and met the definition of haze ($\text{Vis} \leq 10 \text{ km}$ and $\text{RH} \leq 90\%$). Furthermore, as illustrated in Fig. 3, the value of daily averaged AOD in Beijing urban area increased from ~ 0.16 at $\lambda = 500 \text{ nm}$ on 22 September and reached ~ 3.5 on 26 September; the value of AOD increased nearly 22 times from clear day to haze day, and about 17 times larger than that (0.195) of the global mean value of AOD over land studied by Bevan et al. (2012).

3.2 Formation and evolution mechanism of regional haze

3.2.1 Meteorological analysis

The surface weather maps at 05:00 LST from 22–25 September are shown in Fig. 4. Synoptic analyses showed that a slowly migrating anti-cyclone (high-pressure system), which produced clear sky, subsidence, and relatively stagnant conditions (Chen et al., 2003) overlaid Beijing area before 23 September. The edge of a slowly migrating cyclone (which originated in northeastern China) affected Beijing area from 24 September and possibly caused a build-up of pollutants in this region. From China's Fengyun-2 satellite image (<http://www.nmc.gov.cn/publish/satellite/fy2.htm>) (shown by example in Fig. 5), there was no cloud over Beijing area and it provided favorable conditions for photochemical reactions. In addition, the wind speed was relatively low with

A case study in megacity Beijing, China

X. Liu et al.

Title Page

Abstract

Introduction

Conclusions

References

Tables

Figures

◀

▶

◀

▶

Back

Close

Full Screen / Esc

Printer-friendly Version

Interactive Discussion



A case study in megacity Beijing, China

X. Liu et al.

[Title Page](#)[Abstract](#)[Introduction](#)[Conclusions](#)[References](#)[Tables](#)[Figures](#)[⏪](#)[⏩](#)[◀](#)[▶](#)[Back](#)[Close](#)[Full Screen / Esc](#)[Printer-friendly Version](#)[Interactive Discussion](#)

the mean value of 0.9 m s^{-1} from 23–26 September (in Fig. 6), which was consistent with the occurrence of haze episode. On the one hand, low wind speed provided a longer contact time among aerosols and trace gases, and could possibly enhance the formations of new particles (Wang et al., 2006). On the other hand, this stable synoptic condition and calm wind favored the accumulation of the atmospheric pollutants, and horizontal dilution was difficult, ultimately leading to high concentrations of urban pollutants. In addition, the air temperature sharply decreased on 24 September, and the decreasing trend remained till 26 September, which could have caused the lack of the thermal dynamics for the development of the PBL (discussed in Sect. 3.2.3). The RH increased from 24 September, which could have resulted in the hygroscopic growth of aerosol scattering (discussed in Sect. 3.2.5).

3.2.2 Source of pollution

The AOD retrieved from the remote sensing of MODIS by the algorithm introduced by Li et al. (2005) is illustrated in Fig. 7 to depict more detailed features of the spatial distribution of particle pollutants over Jing-Jin-Tang Region. The haze originated from Beijing urban area and then expanded to the surrounding Tianjin, Tangshan, and other cities in Hebei Province, which are heavily populated, urbanized, and industrialized. It implied that this haze case seemed to be a typical build-up of regional pollutants, building up in Beijing firstly and then in other areas later. In addition, the wind speed showed negative correlations with the mass concentration of $\text{PM}_{2.5}$ as discussed in Sect. 3.2.1, which indicates that the haze event might be mainly have formed due to a local pollution source – both direct emissions and secondary transformations.

3.2.3 Development of PBL

The height of PBL was an important parameter, which determined the height of vertical dispersion of air pollutants emitted from the surface of the Earth (Kim et al., 2007).

Low height of PBL would retain the pollutants in the surface layer and make the city shrouded by haze.

Figure 8 is the time-height indication of the normalized LIDAR backscatter signal (in arbitrary units) at 532 nm, and the black line is the height of PBL. With the increase of contamination on the ground, height of PBL significantly decreased. At midday of 23 September, the height of PBL was about 1.5 km, and became 1 km on 24 September, and 0.75 km on 25 September. The development of the PBL was driven by thermal (air temperature) and dynamic (wind speed) factors. On the one hand, lower temperature on 23 September (as shown in Fig. 6) was not conducive to the development of the PBL. On the other hand, low wind speed and thus low entrainment also restricted the development of the PBL. In Fig. 8, the red color indicates heavy aerosol pollution and aerosol mass concentration were increasing with the decreasing PBL height. The solar energy arriving at the Earth was decreasing with the aerosol accumulated in the atmosphere and then the air temperature would drop, which was not conducive to the development of PBL. The feedback effects between the development of PBL and mass loading of aerosols in atmosphere are apparent, and their quantitative relationship is worthy of further study. Aerosols were forced into a very shallow layer due to decreasing height of PBL and lastly resulted in the formation of regional haze. Generally, such external forces such as high wind or rain would be needed to interrupt the further development of this extreme air pollution episode.

3.2.4 New particle formation

Particle size distribution is an important factor determining the amount of visible light scattered by atmospheric aerosols. According to its size distribution, aerosol could be divided into nucleation mode (particles smaller than 10 nm or so), Aitken mode (particles with diameters between 10 and 100 nm or so), accumulation mode (particles diameters from ~ 0.1 to $\sim 2 \mu\text{m}$), and coarse mode (particles diameters larger than $2 \mu\text{m}$). In theory, the contribution of extinction by nucleation mode and coarse mode could be

A case study in megacity Beijing, China

X. Liu et al.

Title Page

Abstract

Introduction

Conclusions

References

Tables

Figures

⏪

⏩

◀

▶

Back

Close

Full Screen / Esc

Printer-friendly Version

Interactive Discussion



ignored regarding visibility impairment, and aerosols in accumulation mode contributed most of the light extinction.

Primary gaseous species such as NO_2 , SO_2 and VOCs could form secondary nitrate, sulfate and organic aerosols in Aitken or nucleation mode through photochemical reaction. This process is called new particle formation or secondary aerosol formation. The criteria of discerning new particle formation events were bursts of the Aitken and nucleation mode particle concentration (Birmili and Wiedensohler, 2000; Liu et al., 2008). With the aerosols in Aitken or nucleation mode aged, the diameter of aerosols grew larger and slid to the accumulation mode, and then aerosol scatter ability increased. That is, new particle formation and the subsequent particle growth or particle aging could result in the enhancing extinction (Wiedensohler et al., 2009).

High temperature and high humidity promoted the photochemical formation of particulate matters. Furthermore, the formation of secondary pollutants would be accelerated in haze days (Xiao and Zhu, 2003; Wang et al., 2006). As illustrated in Fig. 9, the process of new particle formation and evolution, banana-shaped contour, happened on 20, 21, and 22 September. Secondary aerosols showed a remarkably rapid increase from normal to haze days, as depicted by Tan et al. (2009). At noon time with sunny and dry conditions, the photochemical reaction was generally vigorous and new particles formed (Wu et al., 2007). Subsequently, these new particles quickly grew to bigger sizes, and particle cluster was mainly in the accumulation mode in the afternoon. The scattering ability of these aerosols in accumulation was strong and resulted in the deterioration of visibility. Combined with the MODIS observation results discussed in Sect. 3.2.2, the regional haze firstly occurred in Beijing urban area on 23 September, and the secondary aerosol formation was one of the major causes for haze formation. Du et al. (2011) also clarified that secondary aerosol transformation under steady atmospheric conditions played a significant role on the formation of haze in the Yangtze River Delta of China.

A case study in megacity Beijing, China

X. Liu et al.

Title Page

Abstract

Introduction

Conclusions

References

Tables

Figures



Back

Close

Full Screen / Esc

Printer-friendly Version

Interactive Discussion



3.2.5 Impact of hygroscopic growth for aerosol scattering $f(\text{RH})$

Industrial emissions of sulfur and nitrogen oxides could form sulfate, nitrate aerosol particles by photochemical reaction in the atmosphere as new particle formation. Water-soluble ions (such as SO_4^{2-} , NO_3^- , NH_4^+ , and Na^+ , etc.) accounted for ~60 % of the mass of PM_{10} in Beijing (Liu et al., 2009). When RH in the atmosphere was high, these strong hydrophilic aerosols grew in diameter and their ability to scatter light increased (Tang, 1996), which resulted in decreasing the atmospheric visibility (Kaufman and Koren, 2006; Kokkola et al., 2003; Kulmala et al., 1997).

Hygroscopic factor for aerosol scattering $f(\text{RH})$, being the ratio of the aerosol scattering coefficient in wet conditions to that in dry conditions, was calculated by Eq. (3) introduced by Liu et al., (2008, 2010):

$$f(\text{RH}) = \frac{\sigma_{\text{sp}}(\text{RH})}{\sigma_{\text{sp}}(\text{dry})} = \frac{\sigma_{\text{ext}}(\text{RH}) - \sigma_{\text{sg}} - \sigma_{\text{ag}} - \sigma_{\text{ap}}}{\sigma_{\text{sp}}(\text{dry})} \quad (3)$$

where, s and a denote scattering and absorption, and p and g denote particle and gas, respectively.

Figure 10 shows the ratio of wet to dry light scattering acting as a function of RH. The hygroscopic growth factor had the tendency to increase with increasing RH. Usually, the relationship between $f(\text{RH})$ and RH could be fitted by empirical functions: $f(\text{RH}) = 1 + a(\text{RH} 100^{-1})^b$. The curve fitting parameters a and b were 4.34 and 6.72 respectively during the measurement period in this study. The $f(\text{RH})$ at 80 % RH (the mean value for the near-surface atmosphere in the Northern Hemisphere) (Charlson et al., 1991) was 1.97 ± 0.21 with mean and standard deviation. That is, under 80 % RH condition, aerosol scattered nearly two times (more) of light relative to that at dry condition. Moreover, the aerosol scattering generally attributed to nearly 80 % of total atmospheric extinction. So, in case of high RH, its extinction effects would be also amplified with the particles hygroscopic growth. Aerosol hygroscopic properties played an

A case study in megacity Beijing, China

X. Liu et al.

Title Page

Abstract

Introduction

Conclusions

References

Tables

Figures

◀

▶

◀

▶

Back

Close

Full Screen / Esc

Printer-friendly Version

Interactive Discussion



important role on visibility degradation, and the haze was an extreme example of this property.

3.2.6 Visibility empirical equation

Mass concentrations of $PM_{2.5}$ could not properly explain the reasons for reduced visibility because of the fact that haze also associated with the aerosol chemical hygroscopic components and its hygroscopic growth factor $f(RH)$ (Malm and Day, 2001; Cheng et al., 2008a, b; Liu et al., 2008). Aerosol scattering coefficient at dry condition σ_{sp} was calculated by the empirical Eq. (4):

$$\sigma_{sp} = Q_{sp} \times PM_{2.5}. \quad (4)$$

where Q_{sp} is the mass scattering efficiency for $PM_{2.5}$. Taking the RH into account, aerosol scattering coefficient under ambient conditions is derived by Eq. (5):

$$\sigma_{sp}(RH) = Q_{sp} \times PM_{2.5} \times \left(1 + a \times \left(\frac{RH}{100} \right)^b \right) \quad (5)$$

Aerosols that absorbed light were assumed to be hydrophobic, and aerosol absorption coefficient σ_{ap} is illustrated by Eq. (6):

$$\sigma_{ap} = Q_{ap} \times PM_{2.5} \quad (6)$$

where Q_{ap} is the mass absorption efficiency for $PM_{2.5}$.

Additionally, the mean value of $14 Mm^{-1}$ for σ_{ag} during the measurement period was used as the model value for light absorption by gaseous pollutants. Extinction by gas σ_{sg} is assumed to be constant with the value of $10 Mm^{-1}$. Based on the above analysis, atmospheric extinction coefficient $\sigma_{ext}(RH)$ under ambient conditions could be expressed by an approximate Eq. (7):

$$\sigma_{ext}(RH) = \sigma_{sp}(RH) + \sigma_{ap} + \sigma_{sg} + \sigma_{ag} = Q_{sp} \times PM_{2.5} \times \left(1 + a \times \left(\frac{RH}{100} \right)^b \right) + Q_{ap} \times PM_{2.5} + 24 \quad (7)$$

A case study in megacity Beijing, China

X. Liu et al.

Title Page

Abstract

Introduction

Conclusions

References

Tables

Figures

◀

▶

◀

▶

Back

Close

Full Screen / Esc

Printer-friendly Version

Interactive Discussion



A case study in megacity Beijing, China

X. Liu et al.

Title Page

Abstract

Introduction

Conclusions

References

Tables

Figures

◀

▶

◀

▶

Back

Close

Full Screen / Esc

Printer-friendly Version

Interactive Discussion



The values for Q_{sp} and Q_{ap} were $5.3 \text{ m}^2 \text{ g}^{-1}$, and $0.6 \text{ m}^2 \text{ g}^{-1}$ according to the statistics value from the ratio of σ_{sp} and σ_{ap} to $\text{PM}_{2.5}$, respectively, which were omitted in this study. The empirical fitting coefficients a and b were 4.34 and 6.72, respectively, as depicted by Sect. 3.2.5. The atmospheric visibility in unit of km was ultimately converted from this atmospheric extinction coefficient σ_{ext} (RH) by Eq. (1).

The equivalent curve for visibility depending on the mass concentration of $\text{PM}_{2.5}$ and RH is illustrated in Fig. 11. In general, the atmospheric visibility decreased with the increasing mass concentration of $\text{PM}_{2.5}$ and the visibility would decrease sharply with higher RH. The visibility would be less than 3.0 km, and the visibility was only 1.7 km under 80 % RH when the mass concentration of $\text{PM}_{2.5}$ was larger than $200 \mu\text{g m}^{-3}$. Meanwhile, the mass concentration of $\text{PM}_{2.5}$ at dry condition should not exceed $60 \mu\text{g m}^{-3}$ in order to make visibility no less than 10 km (see cross line a and b in Fig. 11). Taking the RH into consideration, the local government should implement more stringent standards for the mass concentration of $\text{PM}_{2.5}$ to meet the same requirements of visibility. For example, the mass concentration of $\text{PM}_{2.5}$ should be less than $30 \mu\text{g m}^{-3}$ when the RH arrives at 80 %. But, daily average $\text{PM}_{2.5}$ concentrations in Beijing ranged from 91 to $169 \mu\text{g m}^{-3}$ (Bergin et al., 2001; Chan et al., 2005; Streets, et al., 2007), and these values had been consistently above the level of $60 \mu\text{g m}^{-3}$. So, it is imperative to control the emission of the atmospheric pollutants aimed to meet the visibility requirements.

4 Conclusion and discussion

In this study, the evolution of haze in Beijing from 20–27 September 2011 was discussed in order to clarify the formation mechanism of this regional haze event. Comprehensive measurements of aerosol characteristics and relevant gas pollutants as well as meteorological conditions were conducted at the PKU urban atmospheric environment monitoring station. Meanwhile, aerosol spatial distribution and the height of PBL were retrieved from the signal of MODIS and LIDAR.

A case study in megacity Beijing, China

X. Liu et al.

Title Page

Abstract

Introduction

Conclusions

References

Tables

Figures



Back

Close

Full Screen / Esc

Printer-friendly Version

Interactive Discussion



At the beginning, plenty of sunlight and higher temperature provided favorable conditions for photochemical reactions and generated more ozone and fine particles. But, a slowly migrating anti-cyclone overlaid northeastern China, with calm wind causing a build-up of pollutants in the Beijing area, and air pollutants wandered inside the source region. Meanwhile, the height of the PBL decreased sharply and pollutants were difficult to spread. Additionally, the hygroscopic components absorbed water vapor and scattered more light with the RH increasing. All of these factors lastly resulted in the formation of haze in Beijing. In summary, haze event in mega-city Beijing was formed mainly due to (1) stable synoptic conditions at the surface and water vapor accumulation in the lower atmosphere; (2) heavy pollution emissions from urban area; (3) gradual reduction of the height of PBL; (4) new particle formation or secondary aerosols transformations; and (5) hygroscopic growth for aerosol scattering. According to the empirical relationship of visibility, $PM_{2.5}$ mass concentration and RH, the mass concentration of $PM_{2.5}$ should be controlled within $60 \mu g m^{-3}$ in order to make visibility no less than 10 km. Taking the RH into consideration, the local government should implement more stringent standards for the mass concentration of $PM_{2.5}$.

The relationship between weather and air pollution was very complicated, and their relationship is an interesting scientific issue that deserved further study. Air pollution was caused by the adverse weather conditions; in other words, unfavorable weather conditions resulted in heavy air pollution. When the concentration of pollutants increased, the amount of solar radiation reaching the ground decreased, which would inevitably lead to lower surface temperature; the then PBL height reduced as well as the RH increased. All of these factors resulted in the visibility degradation. However, when the contamination was light, the sunlight reaching the ground increased and air temperature increased with lower RH and higher PBL, which favored the diffusion of pollutants, and it was not conducive to the formation of haze. Further measurements and modeling studies are needed to investigate the interaction mechanism of air pollution and meteorological conditions. Accordingly, the government should dynamically control the emission of pollutants according to weather conditions. Once on the adverse

weather conditions, the emissions from industrial factories should be strictly controlled, and effective measures to control private car should be taken, and only when atmospheric conditions are good, should normal emissions then be allowed .

Acknowledgements. This work was supported by the National Natural Science Foundation of China (Grant No. 41175018, 41005063 and 20977001). The authors thank Chengcai Li and Yafang Cheng for their useful discussions.

References

- Bell, M. L., Cifuentes, L. A., Davis, D. L., Cushing, E., and Telles, A. G.: Gouveia, N. Environmental health indicators and a case study of air pollution in Latin American cities, *Environ. Res.*, 111, 57–66, 2011.
- Bergin, M. H., Cass, G. R., Xu, J., Fang, C., Zeng, L. M., Yu, T., Salmon, L. G., Kiang, C. S., Tang, X. Y., Zhang, Y. H., and Chameides, W. L.: Aerosol radiative, physical, and chemical properties in Beijing during June 1999, *J. Geophys. Res.*, 106, 17969–17980, 2001.
- Beven, S. L., North, P. R. J., Los, S. O., and Grey, W. M. F.: A global dataset of atmospheric aerosol optical depth and surface reflectance from AATSR, *Remote Sens. Environ.*, 116, 199–210, 2012.
- Birmili, W. and Wiedensohler, A.: New particle formation in the continental boundary layer: meteorological and gas phase parameter influence, *Geophys. Res. Lett.*, 27, 3325–3328, 2000.
- Chameides, W. L., Yu, H., Liu, S. C., Bergin, M., Zhou, X., Mearns, L., Wang, G., Kiang, C. S., Saylor, R. D., Luo, C., Huang, Y., Steiner, A., and Giorgi, F.: Case study of the effects of atmospheric aerosols and regional haze on agriculture: An opportunity to enhance crop yields in China through emission controls?, *Proc. Natl. Acad. Sci. USA*, 96, 13626–13633, 1999.
- Chan, C. Y., Xu, X. D., Li, Y. S., Wong, K. H., Ding, G. A., Chan, L. Y., and Cheng, X. H.: Characteristics of vertical profiles and sources of $PM_{2.5}$, PM_{10} and carbonaceous aerosols in Beijing, *Atmos. Environ.*, 39, 5113–5124. 2005.
- Chen, L. W. A., Chow, J. C., Doddridge, B. G., Dickerson, R. R., Ryan, W. F., and Mueller, P. K.: Analysis of a summertime $PM_{2.5}$ and haze episode in the mid-Atlantic region, *J. Air Waste Manage. Assoc.*, 53, 946–956, 2003.

A case study in megacity Beijing, China

X. Liu et al.

Title Page

Abstract

Introduction

Conclusions

References

Tables

Figures

◀

▶

◀

▶

Back

Close

Full Screen / Esc

Printer-friendly Version

Interactive Discussion



A case study in megacity Beijing, China

X. Liu et al.

Title Page

Abstract

Introduction

Conclusions

References

Tables

Figures

◀

▶

◀

▶

Back

Close

Full Screen / Esc

Printer-friendly Version

Interactive Discussion



Cheng, Y. F., Eichler, H., Wiedensohler, A., Heintzenberg, J., Zhang, Y. H., Hu, M., Herrmann, H., Zeng, L. M., Liu, S., Gnauk, T., Brüggemann, E., and He, L. Y.: Mixing state of elemental carbon and non-light-absorbing aerosol components derived from in situ particle optical properties at Xinken in Pearl River Delta of China, *J. Geophys. Res.*, 111, D20204, doi:10.1029/2005JD006929, 2006.

Cheng, Y. F., Wiedensohler, A., Eichler, H., Su, H., Gnauk, T., Brüggemann, E., Herrmann, H., Heintzenberg, J., Slanina, J., Tuch, T., Hu, M., and Zhang, Y. H.: Aerosol optical properties and related chemical apportionment at Xinken in Pearl River Delta of China, *Atmos. Environ.*, 42, 6351–6372, 2008a.

Cheng, Y. F., Wiedensohler, A., Eichler, H., Heintzenberg, J., Tesche, M., Ansmann, A., Wendisch, M., Su, H., Althausen, D., Herrmann, H., Gnauk, T., Brüggemann, E., Hu, M., and Zhang, Y. H.: Relative humidity dependence of aerosol optical properties and direct radiative forcing in the surface boundary layer at Xinken in Pearl River Delta of China: An observation based numerical study, *Atmos. Environ.*, 42, 6373–6397, 2008b.

Deng, X., Tie, X., Wu, D., Zhou, X., Bi, X., Tan, H., Li, F., and Jiang, C.: Long-term trend of visibility and its characterization in the Pearl River Delta (PRD) region, China. *Atmos. Environ.*, 42, 1424–1435, 2008.

Du, H. H., Kong, L. D., Cheng, T. T., Chen, J. M., Du, J. F., Li, L., Xia, X. A., Leng, C. P., and Huang, G. H.: Insights into summertime haze pollution events over Shanghai based on online water-soluble ionic composition of aerosols, *Atmos. Environ.*, 45, 5131–5137, 2011.

Hayden, K. L., Anlauf, K. G., Hoff, R. M., Strapp, J. W., Bottenheim, J. W., Wiebe, H. A., Froude, F. A., and Martin, J. B.: The vertical chemical and meteorological structure of the boundary layer in the Lower Fraser Valley during Pacific 93, *Atmos. Environ.*, 31, 2089–2105, 1997.

He, K., Yang, F., Ma, Y., Zhang, Q., Yao, X., Chan, C. K., Cadle, S., Chan, T., and Mulawa, P.: The characteristics of PM_{2.5} in Beijing, China. *Atmos. Environ.*, 35, 4959–4970, 2001.

Huebert, B. J., Bates, T., Russell, P. B., Shi, G. Y., Kim, Y. J., Kawamura, K., Carmichael, G., and Nakajima, T.: An overview of ACE-Asia: Strategies for quantifying the relationships between Asian aerosols and their climatic impacts, *J. Geophys. Res.*, 108, 8633, doi:10.1029/2003JD003550, 2003.

Kim, S. W., Yoon, S. C., Won, J. G., and Choi, S. C.: Ground-based remote sensing measurements of aerosol and ozone in an urban area: a case study of mixing height evolution and its effect on ground-level ozone concentrations, *Atmos. Environ.*, 41, 7069–7081, 2007.

A case study in megacity Beijing, China

X. Liu et al.

Title Page

Abstract

Introduction

Conclusions

References

Tables

Figures

◀

▶

◀

▶

Back

Close

Full Screen / Esc

Printer-friendly Version

Interactive Discussion



- Koschmieder, H.: Theorie der horizontalen Sichtweite, Beiträge zur Physik der freien Atmosphäre, 12, 33–53, 1924.
- Lee, D. O.: Trends in summer visibility in London and Southern England 1962–1979, Atmos. Environ., 17, 151–159, 1983.
- 5 Li, C., Lau, K. H., Mao, J., and Chu, D. A.: Retrieval, validation and application of the 1-km aerosol optical depth from MODIS measurements over Hong Kong. IEEE Trans, Geosci. Remote Sens., 43, 2650–2658, 2005.
- Liu, S., Hu, M., Wu, Z. J., Wehner, B., Wiedensohler, A., and Cheng, Y. F.: Aerosol number size distribution and new particle formation at a rural/coastal site in Pearl River Delta (PRD) of China, Atmos. Environ., 42, 6275–6283, 2008.
- 10 Liu, X. G., Cheng, Y. F., Zhang, Y. H., Jung, J. S., Sugimoto, N., Chang, S.-Y., Kim, Y. J., Fan, S. J., and Zeng, L. M.: Influences of relative humidity and particle chemical composition on aerosol scattering properties during the 2006 PRD campaign, Atmos. Environ., 42, 1525–1536, 2008.
- 15 Liu, X. G., Zhang, Y. H., Jung, J. S., Gu, J. W., Li, Y. P., Guo, S., Chang, S. -Y., Yue, D., Lin, P., Kim, Y. J., Hu, M., Zeng, L. M., and Zhu. T.: Research on Aerosol Hygroscopic Properties by Measurement and Model during the 2006 CAREBeijing Campaign, J. Geophys. Res., 114, D00G16, doi:10.1029/2008JD010805, 2009.
- Liu, X. G., Zhang, Y. H., Wen M. T., Wang, J. L., Jung, J. S. Chang, S.-Y., Hu, M., Zeng, L. M., and Kim, Y. J.: A Closure Study of Aerosol Hygroscopic Growth Factor during the 2006 PRD Campaign, Adv. Atmos. Sci., 27, 947–956, doi:10.1007/s00376-009-9150-z, 2010.
- 20 Malm, W. C. and Day, D. E.: Estimates of aerosol species scattering characteristics as a function of relative humidity, Atmos. Environ., 35, 2845–2860, 2001.
- McNulty, R. P.: The effect of air pollutants on visibility in fog and haze at New York city, Atmos. Environ., 2, 625–628, 1968.
- 25 Melfi, S. H., Spinhirne, J. D., Chou, S. H., and Palm, S. P.: Lidar observation of vertically organized convection in the planetary boundary layer over the ocean, J. Appl. Meteorol. Clim., 24, 806–821, 1985.
- Mukherjee, P. and Viswanathan S.: Contributions to CO concentrations from biomass burning and traffic during haze episodes in Singapore, Atmos. Environ., 35, 715–725, 2001.
- 30 Quinn, P. K. and Bates, T.: North American, Asian, and Indian haze: Similar regional impacts on climate?, Geophys. Res. Lett., 30, 1555, doi:10.1029/2003GL016934, 2003.

A case study in megacity Beijing, China

X. Liu et al.

Title Page

Abstract

Introduction

Conclusions

References

Tables

Figures

◀

▶

◀

▶

Back

Close

Full Screen / Esc

Printer-friendly Version

Interactive Discussion



- Quinn, P. K., Coffman, D. J., Bates, T. S., Miller, T. L., Johnson, J. E., Welton, E. J., Neususs, C., Miller, M., and Sheridan, P. J.: Aerosol optical properties during INDOEX 1999: Means, variability, and controlling factors. *J. Geophys. Res.*, 107, 8020, doi:10.1029/2000JD000037, 2002.
- 5 Schichtel, B. A., Husar, R. B., Falke, S. R., and Wilson, W. E.: Haze trends over the United States, 1980–1995, *Atmos. Environ.*, 35, 5205–5210, 2001.
- Seinfeld, J. H. and Pandis, S. N.: *Atmospheric Chemistry and Physics*, in: *Air Pollution to Climate Change*, 2nd Edn., Wiley, J. & Sons, Inc., New York, USA, 2006.
- Streets, D. G., Fu, J. S., Jang, C. J., Hao, J. M., He, K. B., Tang, X. Y., Zhang, Y. H., Wang, Z. F.,
10 Li, Z. P., Zhang, Q., Wang, L. T., Wang, B. Y., and Yu, C.: Air quality during the 2008 Beijing Olympic Games, *Atmos. Environ.*, 41, 480–492, 2007.
- Sugimoto, N., Nishizawa, T., Liu, X. G., Matsui, I., Shimizu, A., Zhang, Y. H., Kim, Y. J., Li, R. H., and Liu, J.: Continuous observations of aerosol profiles with a two-wavelength Mie-scattering lidar in Guangzhou in PRD2006, *J. Appl. Meteorol. Clim.*, 48, 1822–1830, 2009.
- 15 Sun, Y. L., Zhuang, G. S., Wang, Y., Han, L. H., Guo, J. H., Dan, M., Zhang, W. J., Wang, Z. F., and Hao, Z. P.: The air-borne particulate pollution in Beijing-Concentration, composition, distribution and sources, *Atmos. Environ.*, 38, 5991–6004, 2004.
- Sun, Y. L., Zhuang, G. S., Tang, A. H., Wang, Y., and An, Z. S.: Chemical characteristics of PM_{2.5} and PM₁₀ in haze-fog Episodes in Beijing, *Environ. Sci. Technol.*, 40, 3148–3155, 2006.
- 20 Tan, J. H., Duan, J. C., Chen, D. H., Wang, X. H., Guo, S. J., Bi, X. H., Sheng, G. Y., He, K. B., and Fu, J. M.: Chemical characteristics of haze during summer and winter in Guangzhou, *Atmos. Res.*, 94, 238–245, 2009.
- Tie, X. X., Wu, D., and Brasseur, G.: Lung cancer mortality and exposure to atmospheric aerosol particles in Guangzhou, China, *Atmos. Environ.*, 43, 2375–2377, 2009.
- 25 Wang, Y., Zhuang, G. S., Sun, Y. L., and An, Z. S.: The variation of characteristics and formation mechanisms of aerosols in dust, haze, and clear days in Beijing, *Atmos. Environ.*, 40, 6579–6591, 2006.
- Wiedensohler, A., Cheng, Y. F., Nowak, A., Wehner, B., Achtert, P., Berghof, M., Birmili, W., Wu, Z. J., Hu, M., Zhu, T., Takegawa, N., Kita, K., Kondo, Y., Lou, S. R., Hofzumahaus, A., Holland, F., Wahner, A., Gunthe, S. S., Rose, D., Su, H., and Poeschl, U.: Rapid aerosol particle growth and increase of cloud condensation nucleus activity by secondary aerosol

A case study in megacity Beijing, China

X. Liu et al.

[Title Page](#)[Abstract](#)[Introduction](#)[Conclusions](#)[References](#)[Tables](#)[Figures](#)[⏪](#)[⏩](#)[◀](#)[▶](#)[Back](#)[Close](#)[Full Screen / Esc](#)[Printer-friendly Version](#)[Interactive Discussion](#)

formation and condensation: a case study for regional air pollution in northeastern China, *J. Geophys. Res.*, 114, D00G08, doi:10.1029/2008JD010884, 2009.

Wu, D., Tie, X., Li, C., Ying, Z., Lau, A. K.-H., Huang, J., Deng, X., and Bi, X.: An extremely low visibility event over the Guangzhou region: a case study, *Atmos. Environ.*, 39, 6568–6577, 2005.

Wu, D., Bi, X., Deng, X., Li, F., Tan, H., Liao, G., and Huang, J.: Effects of atmospheric haze on the deterioration of visibility over the Pearl River Delta, *Acta Meteorol. Sin.*, 64, 510–517, 2006.

Wu, Z., Hu, M., Liu, S., Wehner, B., Bauer, S., Maßling, A., Wiedensohler, A., Petäjä, T., Dal-Maso, M., and Kulmala, M.: New particle formation in Beijing, China: Statistical analysis of a 1-year dataset, *J. Geophys. Res.*, 112, D09209, doi:10.1029/2006JD007406, 2007.

Xiao, F., Brajer, V., and Mead, R. W.: Blowing in the wind: the impact of China's Pearl River Delta on Hong Kong's air quality, *Sci. Total Environ.*, 367, 96–111, 2006.

Xiao, H. and Zhu, B.: Modelling study of photochemical ozone creation potential of non-methane hydrocarbon, *Water Air Soil Poll.*, 145, 3–16, 2003.

Yadav, A. K., Kumar, K., Kasim, A., Singh, M. P., Parida, S. K., and Sharan, M.: Visibility and incidence of respiratory diseases during the 1998 haze episode in Brunei Darussalam, *Pure Appl. Geophys.*, 160, 265–277, 2003.

Zhang, Y. H., Hu, M., Zhong, L. J., Wiedensohler, A., Liu, S. C., Andreae, M. O., Wang, W., and Fan, S. J.: Regional integrated experiments on air quality over Pearl River Delta 2004 (PRIDE-PRD2004): Overview, *Atmos. Environ.*, 42, 6157–6173, 2008.

Table 1. Overview of instruments involved in this study.

Instrument	Parameter	Manufacturer Model	Calibration (nm)	Wavelength
Visibility meter	Atmospheric Extinction coefficient	Vaisala FD12	Before and after the campaign	875
Integrating Nephelometer	Aerosol scattering coefficient	Ecotech M9003	Zero, span check(CO ₂) every day	525
MAAP	Aerosol absorption coefficient	Thermo. Electron. Caruso 5012	Zero, flow-rate check at the start/end	670
Sunphotometer	Aerosol optical depth	Solar light Inc. Microtops Π	/	380, 500, 675, 870, 1020
TEOM	PM _{2.5}	Thermo. Electron. 1400a	/	/
Relative humidity sensor	RH	Vaisala HMP45	/	/
Pulsed Fluorescence SO ₂ Analyzer	SO ₂	Thermo. Electron. 43iTL	Zero, span check every day	/
Chemiluminescence NO-NO ₂ -NO _x Analyzer	NO-NO ₂ -NO _x	Thermo. Electron. 42iTL	Zero, span check every day	/
UV Photometric O ₃ Analyzer	O ₃	Thermo. Electron. 49i	Zero, span check every day	/
Gas Filter Correlation CO Analyzer	CO	Thermo. Electron. 48iTL	Zero, span check every day	/
LIDAR	PBL height	NIES ¹	/	525
SMPS	Particle size distribution (2.5 ~ 1000 nm)	TSI Com. 3936	/	/
APS	Particle size distribution (0.5 ~ 20 μm)	TSI Com. 3321	/	/

¹ NIES: National Institute for Environmental Studies, Japan.

A case study in megacity Beijing, China

X. Liu et al.

Title Page

Abstract

Introduction

Conclusions

References

Tables

Figures

◀

▶

◀

▶

Back

Close

Full Screen / Esc

Printer-friendly Version

Interactive Discussion



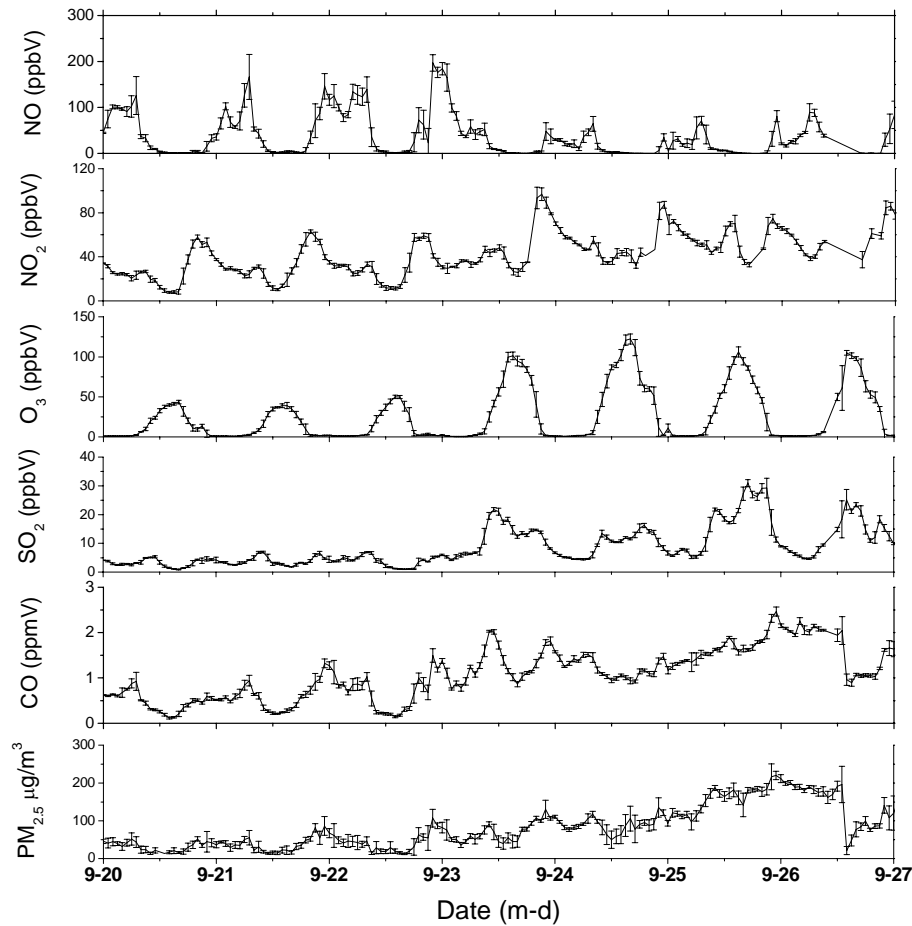


Fig. 1. Time series of observed NO, NO₂, SO₂, O₃, CO, and PM_{2.5} in Beijing from 20–27 September 2011.

A case study in megacity Beijing, China

X. Liu et al.

Title Page

Abstract Introduction

Conclusions References

Tables Figures

◀ ▶

◀ ▶

Back Close

Full Screen / Esc

Printer-friendly Version

Interactive Discussion



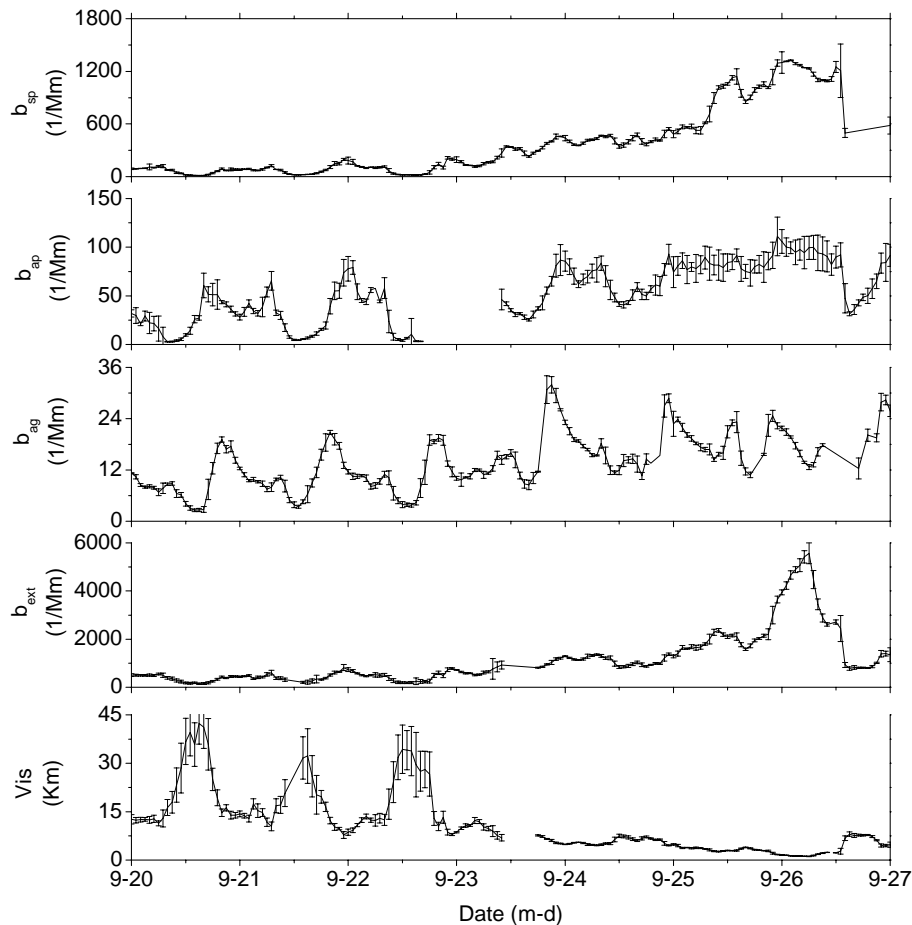


Fig. 2. Time series of measured aerosol scattering coefficient b_{sp} , aerosol absorption coefficient b_{ap} , absorption coefficient by NO_2 b_{ag} , atmospheric extinction coefficient b_{ext} , and atmospheric visibility (vis) in Beijing from 20–27 September 2011.

A case study in megacity Beijing, China
X. Liu et al.

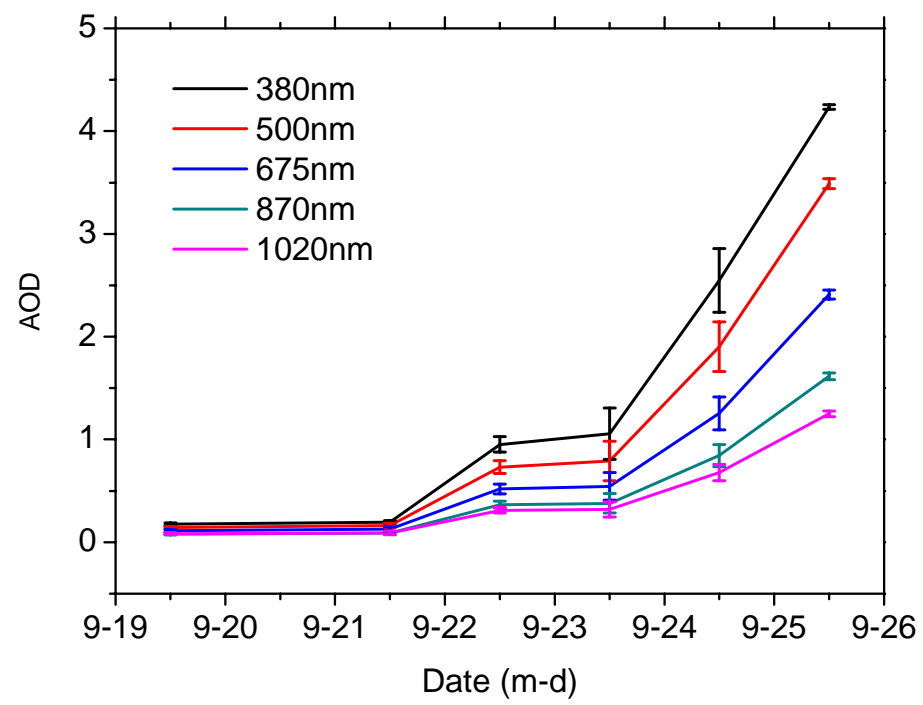


Fig. 3. Temporal series of aerosol optical depth measured by sunphotometer in Beijing.

Title Page

Abstract Introduction

Conclusions References

Tables Figures

◀ ▶

◀ ▶

Back Close

Full Screen / Esc

Printer-friendly Version

Interactive Discussion



A case study in megacity Beijing, China

X. Liu et al.

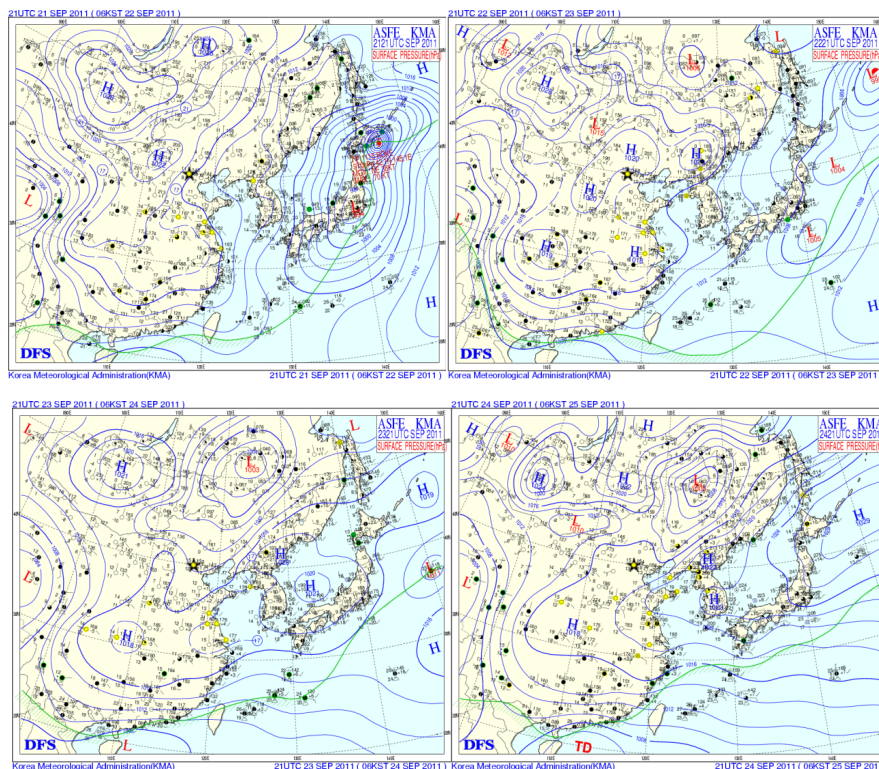


Fig. 4. Weather maps on the surface at (a) 05:00 LST September 22; (b) 05:00 LST 23 September; (c) 05:00 LST 24 September; and (d) 05:00 LST 25 September. Black star denotes measurement site.

Title Page

Abstract

Introduction

Conclusions

References

Tables

Figures

◀

▶

◀

▶

Back

Close

Full Screen / Esc

Printer-friendly Version

Interactive Discussion



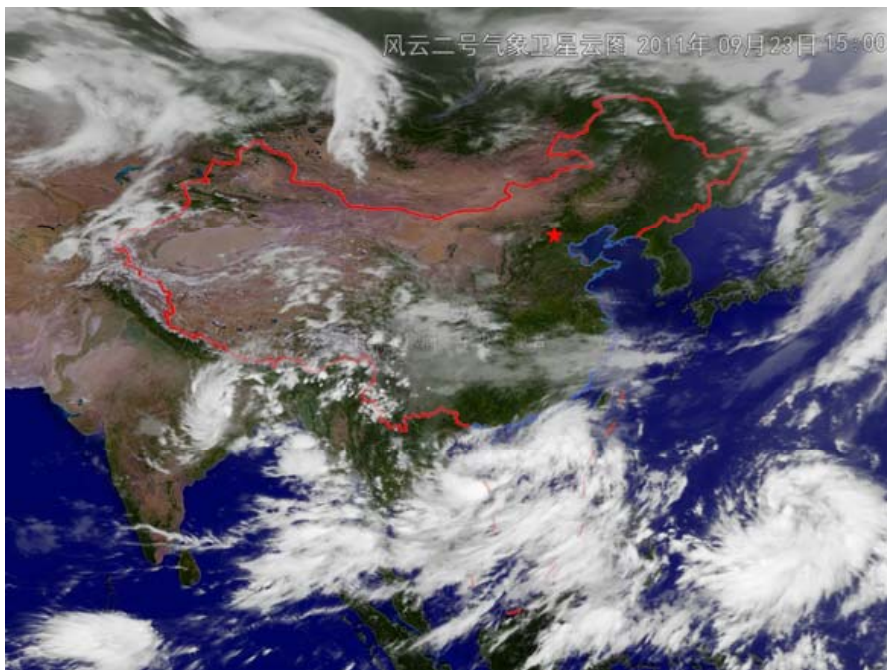


Fig. 5. Example of satellite maps during haze. Red star denotes measurement site.

A case study in megacity Beijing, China

X. Liu et al.

Title Page

Abstract

Introduction

Conclusions

References

Tables

Figures

◀

▶

◀

▶

Back

Close

Full Screen / Esc

Printer-friendly Version

Interactive Discussion



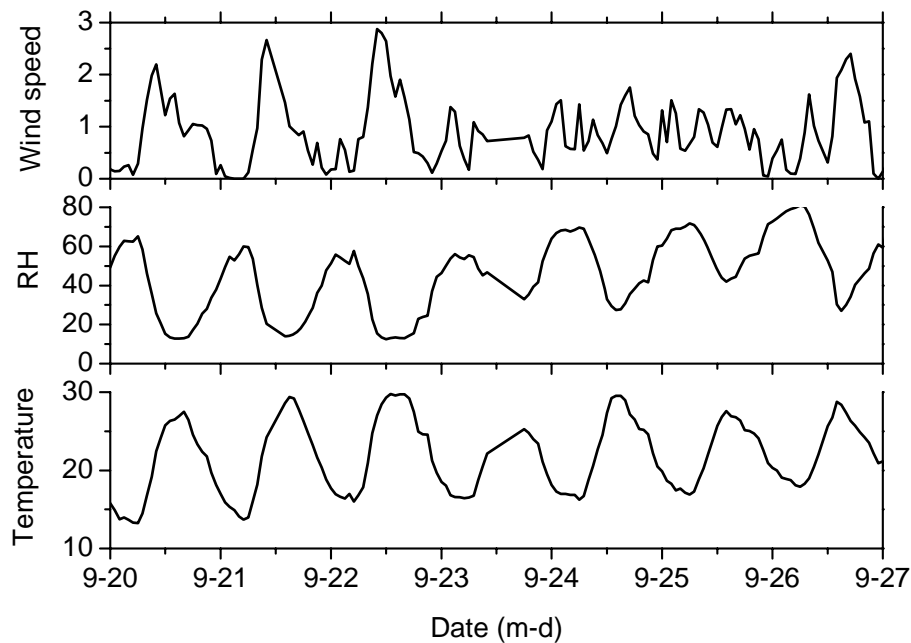


Fig. 6. Time series of meteorological parameter during haze.

A case study in megacity Beijing, China

X. Liu et al.

Title Page

Abstract Introduction

Conclusions References

Tables Figures

◀ ▶

◀ ▶

Back Close

Full Screen / Esc

Printer-friendly Version

Interactive Discussion



A case study in megacity Beijing, China

X. Liu et al.

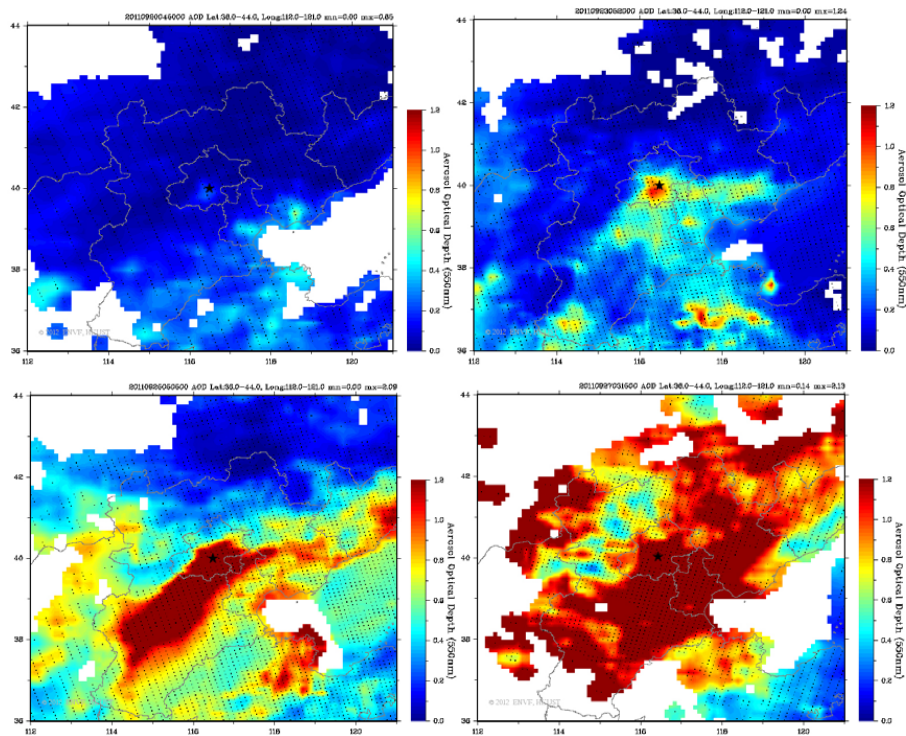


Fig. 7. Aerosol optical depth measured by MODIS on (a) September 20, (b) 23 September, (c) 25 September, and (d) 27 September. Black star denotes measurement site.

Title Page

Abstract

Introduction

Conclusions

References

Tables

Figures

◀

▶

◀

▶

Back

Close

Full Screen / Esc

Printer-friendly Version

Interactive Discussion



A case study in megacity Beijing, China

X. Liu et al.

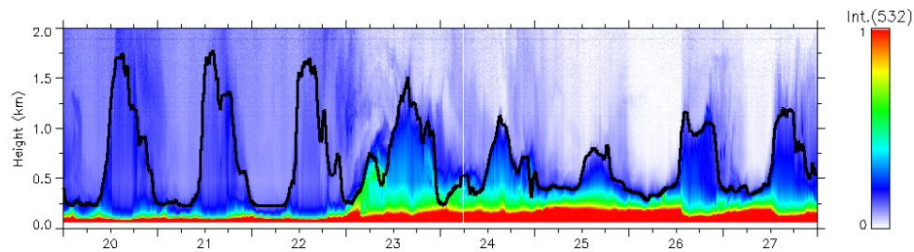


Fig. 8. Time-height indications of the normalized LIDAR backscatter signal in arbitrary units at 532 nm. The black line is the height of the PBL.

[Title Page](#)[Abstract](#)[Introduction](#)[Conclusions](#)[References](#)[Tables](#)[Figures](#)[◀](#)[▶](#)[◀](#)[▶](#)[Back](#)[Close](#)[Full Screen / Esc](#)[Printer-friendly Version](#)[Interactive Discussion](#)

A case study in megacity Beijing, China

X. Liu et al.

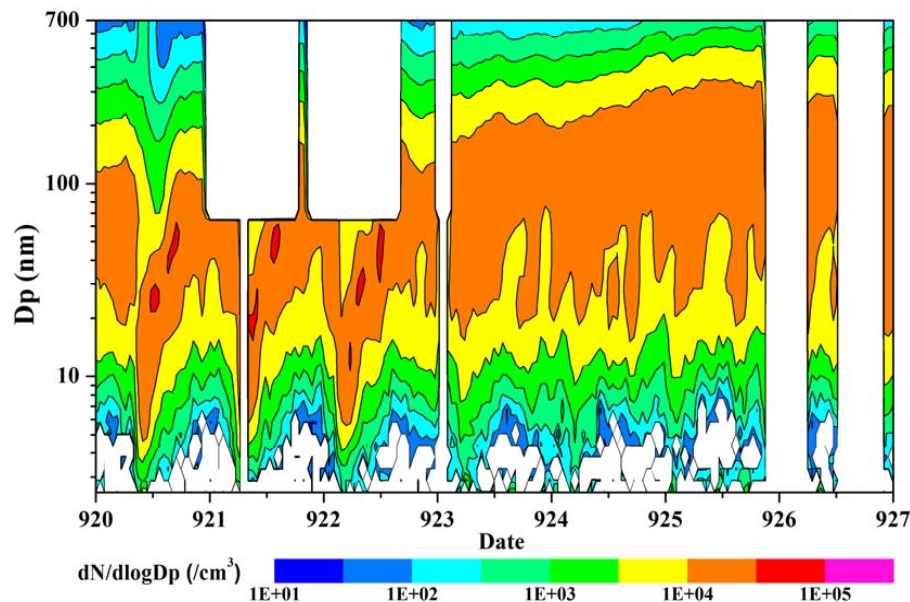


Fig. 9. Temporal variance of particle size distribution from 20–27 September. Empty space denotes lack of measurements.

[Title Page](#)[Abstract](#)[Introduction](#)[Conclusions](#)[References](#)[Tables](#)[Figures](#)[◀](#)[▶](#)[◀](#)[▶](#)[Back](#)[Close](#)[Full Screen / Esc](#)[Printer-friendly Version](#)[Interactive Discussion](#)

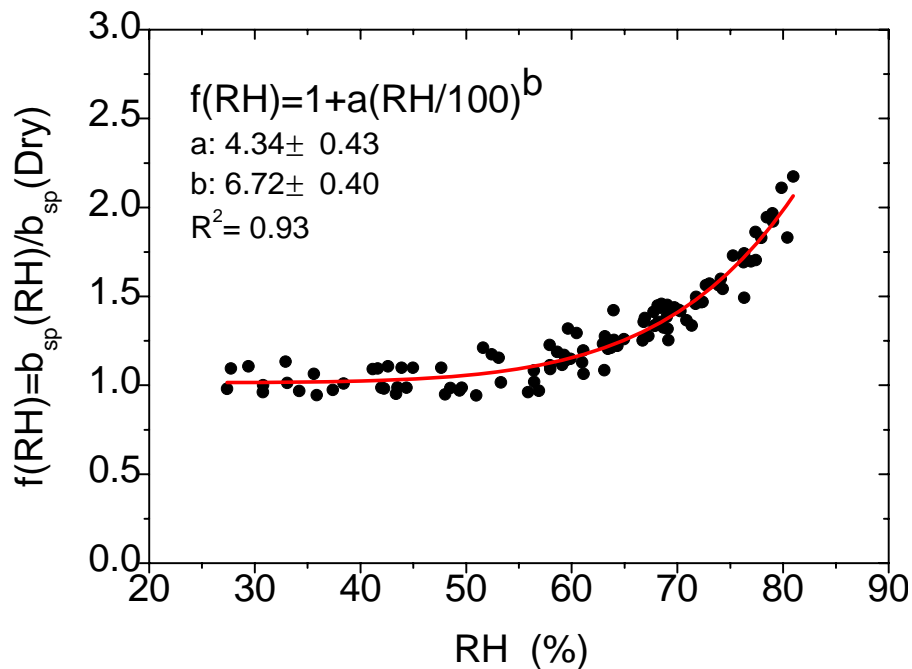


Fig. 10. Hygroscopic growth for aerosol scattering $f(\text{RH})$ as a function of RH with curve fitting. Scattered dots are the measured $f(\text{RH})$, and the line is the empirical fitting curve.

A case study in megacity Beijing, China

X. Liu et al.

Title Page

Abstract

Introduction

Conclusions

References

Tables

Figures

◀

▶

◀

▶

Back

Close

Full Screen / Esc

Printer-friendly Version

Interactive Discussion



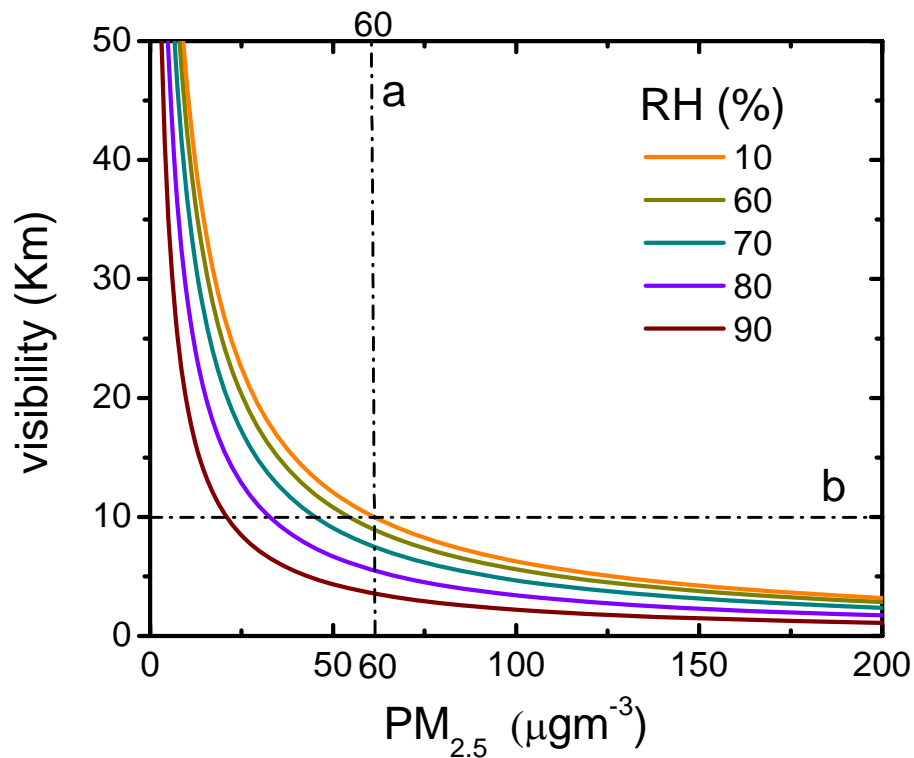


Fig. 11. The equivalent curve for visibility depending on the mass concentration of $PM_{2.5}$ and relative humidity. Line **(b)** is the standard for visibility equal to 10 km, and line **(a)** is the limit for mass concentration of $PM_{2.5}$ under dry conditions ($RH = 10\%$).